

Vortices with antiferromagnetic cores in the SO(5) model of high temperature superconductivity

S. Alama¹, A.J. Berlinsky², L. Bronsard¹, and T. Giorgi¹

¹*Department of Mathematics and Statistics, McMaster University,
Hamilton, Ontario, Canada L8S 4M1*

²*Department of Physics and Astronomy, McMaster University,
Hamilton, Ontario, Canada L8S 4M1*

(November 1, 2019)

We consider the problem of superconducting Ginzburg-Landau (G-L) vortices with antiferromagnetic cores which arise in Zhang's SO(5) model of antiferromagnetism (AF) and high temperature superconductivity (SC). This problem was previously considered by Arovas *et al.* who constructed approximate "variational" solutions, in the large κ limit, to estimate the domain of stability of such vortices in the temperature-chemical potential phase diagram. By solving the G-L equations numerically for general κ , we show that the amplitude of the antiferromagnetic component at the vortex core decreases to zero continuously at a critical value of the AF-SC anisotropy ($g \approx 0.25$) which is essentially independent of κ for large κ . The magnetic field profile, the vortex line energy and the value of the B-field at the center of the vortex core, as functions of anisotropy are also presented.

I. INTRODUCTION

Zhang [1] has proposed a model which attempts to relate the antiferromagnetism and d-wave superconductivity observed in the high T_c cuprates by a symmetry principle. In this model, the Neel vector, \mathbf{m} , which is the order parameter for antiferromagnetism, and the real and imaginary parts of the complex superconducting order parameter ψ form the five components of a so-called "superspin" vector which transforms under the group SO(5). This symmetry is explicitly broken by an anisotropy which favors antiferromagnetism (AF) for the undoped compounds (which have one unpaired electron spin per site). The anisotropy can be varied by a chemical potential term which adds holes (or equivalently removes electron spins). For sufficiently large chemical potential, the anisotropy changes sign stabilizing the superconducting (SC) state.

A straightforward consequence of this model, as noted by Zhang [1], is that, close to the SC-AF phase boundary, vortices in the superconducting state should have antiferromagnetic cores. The idea is simply that, for small anisotropy, it is easier to simply rotate the order parameter in the core into the AF direction than it is to reduce its amplitude to zero. Arovas *et al.* [2], following Zhang's suggestion, calculated the approximate domain of stability of vortices with AF cores, within Ginzburg-Landau theory, in the temperature-chemical potential plane. Their calculation compared the energies of two variational solutions for the behavior of the superspin vector, (1) the function $\tanh(r/\xi)$ for the magnitude of the SC order parameter, representing a vortex with a normal core and (2) a vector making an angle $\theta(r) = (\pi/2)\exp(-r/\ell)$ toward the AF direction from the SC direction. The contribution of the vector potential to the free energy was ignored, as is appropriate for the extreme type-II limit ($\kappa \rightarrow \infty$). By comparing

the energies of these two configurations, minimized with respect to ξ and ℓ , as a function of the G-L parameters, Arovas and coworkers located a boundary within the SC region of the phase diagram, where vortex core solutions (1) and (2) exchange stability. If these solutions were exact, the implication would be that the amplitude of antiferromagnetism in the core changes discontinuously across this boundary.

In this paper we consider the full numerical solution of the coupled non-linear Ginzburg-Landau equations for vortices in the phenomenological SO(5) model, including the vector potential. We calculate the AF and SC order parameter profiles and the magnetic field profiles as functions of distance from the core for general κ and anisotropy. We find a much broader range of stability for vortices with AF cores than was found by Arovas *et al.* We also find that the amplitude of the AF component in the core falls continuously to zero with increasing chemical potential as the phase boundary for normal cores is approached, and we calculate the critical value of the anisotropy(chemical potential) where this transition occurs for a range of κ , including $\kappa = \infty$. We also obtain the dependence of the vortex line energy and the field at the core on κ in the large κ limit for AF and normal cores. Our results allow us to conclude that both H_{c1} and H_{c2} increase with increasing anisotropy as the cores become less antiferromagnetic.

II. FREE ENERGY

We consider the following Ginzburg-Landau free energy for superspin vector $\mathbf{n} = (\psi_1, m_1, m_2, m_3, \psi_2)$ with vector potential \mathbf{A} ,

$$\frac{1}{2} \int \left\{ f_0 + a|\mathbf{n}|^2 + \frac{1}{2}b|\mathbf{n}|^4 - \tilde{g}|\mathbf{m}|^2 + \frac{\hbar^2}{2m^*} \left| \left(\frac{1}{i} \nabla - \frac{e^*}{\hbar c} \mathbf{A} \right) \psi \right|^2 + \frac{\hbar^2}{2m^*} |\nabla \mathbf{m}|^2 + \frac{1}{8\pi} |\nabla \times \mathbf{A}|^2 \right\} dx \quad (1)$$

The anisotropy is measured by $\tilde{g} = 4\chi(\mu_c^2 - \mu^2)$, where μ denotes the chemical potential.

We introduce a non-dimensional form of the energy. In these units the penetration depth $\lambda = 1$, and the correlation length ξ and GL parameter κ are related via $\xi = \kappa^{-1}$. More precisely, we let

$$\mathbf{x} = \lambda \hat{\mathbf{x}}, \quad \psi = \sqrt{\frac{|a|}{b}} \hat{\psi}, \quad \mathbf{m} = \sqrt{\frac{|a|}{b}} \hat{\mathbf{m}}, \quad \mathbf{A} = \frac{c\hbar}{\lambda e^*} \hat{\mathbf{A}}, \quad (2)$$

where

$$\lambda = \sqrt{\frac{m^* b c^2}{4\pi |a| (e^*)^2}} \quad \text{and} \quad \xi = \sqrt{\frac{\hbar^2}{2m^* |a|}}. \quad (3)$$

Then the free energy becomes (up to a factor of $\frac{\hbar^2 |a|}{2m^* b}$)

$$\frac{1}{2} \int \left\{ \frac{\kappa^2}{2} (1 - |\hat{\mathbf{n}}|^2)^2 + g\kappa^2 |\hat{\mathbf{m}}|^2 + \left| \left(\frac{1}{i} \nabla - \hat{\mathbf{A}} \right) \hat{\psi} \right|^2 + |\nabla \hat{\mathbf{m}}|^2 + |\nabla \times \hat{\mathbf{A}}|^2 \right\} d\hat{\mathbf{x}}. \quad (4)$$

The anisotropy term is regulated by a new constant g ,

$$g = \frac{\tilde{g}}{a} = \frac{4\chi(\mu^2 - \mu_c^2)}{|a|}, \quad (5)$$

which is positive when superconductivity is preferred in the bulk ($\mu > \mu_c$). For convenience, we drop the hats on non-dimensional quantities in the following.

A. Vortex solutions

We now seek vortex solutions in the plane, in other words free energy minimizers of the form $\psi(x) = f(r)e^{i\theta}$, $\mathbf{m}(\mathbf{x}) = m(r)\hat{\mathbf{m}}$ with $\hat{\mathbf{m}}$ a fixed unit vector, and $\mathbf{A}(x) = [S(r)/r^2](-y, x) = [S(r)/r]\hat{\theta}$. In addition we require that $f(0) = 0$, $f(r \rightarrow \infty) \rightarrow 1$, $m(r \rightarrow \infty) \rightarrow 0$, $S(0) = 0$, and $S(r \rightarrow \infty) \rightarrow 1$. Note that requiring \mathbf{m} to lie in a fixed direction does not restrict the minimization problem, since spatial variations in direction of \mathbf{m} will increase the free energy. With this ansatz, the energy takes the form:

$$\begin{aligned} \mathcal{E} = \pi \int_0^\infty \{ & (f'(r))^2 + \left(\frac{S'(r)}{r} \right)^2 \\ & + \frac{(1-S)^2 f^2}{r^2} + (m'(r))^2 + \kappa^2 g m^2 \\ & + \kappa^2 (1 - f^2 - m^2)^2 \} r dr. \end{aligned} \quad (6)$$

f, S, m satisfy the following Euler-Lagrange equations:

$$-f''(r) - \frac{1}{r} f'(r) + \frac{(1-S(r))^2}{r^2} f$$

$$-\kappa^2 (1 - f^2 - m^2) f = 0, \quad (7)$$

$$-S''(r) + \frac{1}{r} S'(r) - (1-S)f^2 = 0, \quad (8)$$

$$\begin{aligned} -m''(r) - \frac{1}{r} m'(r) + g\kappa^2 m \\ -\kappa^2 (1 - f^2 - m^2) m = 0. \end{aligned} \quad (9)$$

By linearization at $r = 0$ we obtain the standard properties for vortex solutions: [3,4] $f(r) \sim \alpha r$ and $S(r) \sim \beta r^2$ near $r = 0$. Unconstrained minimization also yields $m'(0) = 0$. Using Theorem 7.2 in Jaffe–Taubes [5] we see that f, S, m approach their asymptotic limits $r \rightarrow \infty$ exponentially. In addition, $f(r)$ and $S(r)$ are monotonically increasing, while the z -component of the local field $h(r) = S'(r)/r$ is monotonically decreasing. The AF order parameter $m(r)$ is either positive and monotonically decreasing or identically zero. [6] These properties are illustrated in Figure 1.

The results shown in Figure 1 and elsewhere in this paper come from numerical solutions of (7)–(9). Our technique is to find free energy minimizers by computing a negative gradient flow for a discretized free energy. We approximate the improper integral in \mathcal{E} by an integral over a finite interval, large compared to the fundamental scales ($\lambda = 1$ and $\xi = \kappa^{-1}$) in the problem. We set a fixed boundary condition for f, S, m at the right endpoint, equal to their asymptotic values. We then use finite elements to discretize the integral, with a fine mesh concentrated at the vortex core. For example, in Figure 3 we divide the r -interval $[0, 10]$ by 350 grid points, with 300 points lying in $[0, 2]$. We choose standard linear

elements, except in the first interval near 0, where the behavior of $S(r)$ is known to be quadratic.

We then explicitly calculate the gradient of the discretized energy with respect to the coefficients $(f_k), (S_k), (m_k)$ of the base elements. To find the minimal configuration, we start with some initial data, and flow the coefficient vector $(f_k), (S_k), (m_k)$ against the gradient until an equilibrium is found. To solve the gradient flow numerically, we use a code developed by Dr. N. Carlson of Los Alamos National Laboratory, which he very kindly made available to us. In this code the ODE is solved by an implicit method, using second order backwards differences. At each time step the resulting nonlinear system is solved by a modified Newton method, and the time step is chosen based on estimates of the local truncation error.

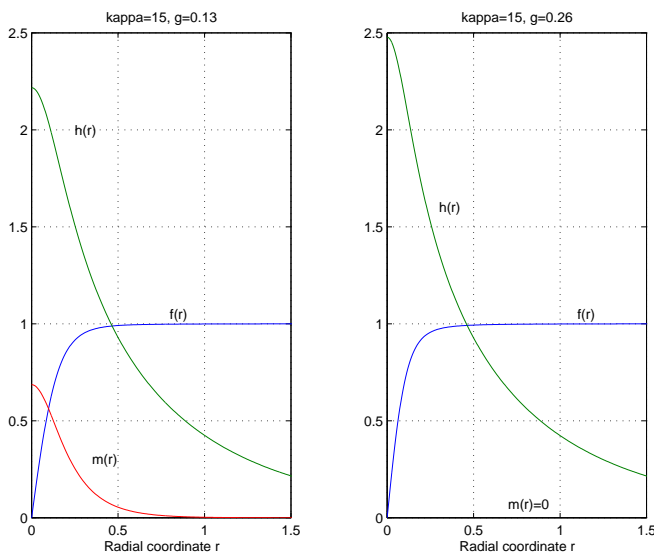


FIG. 1. Typical profiles for f, h, m at $\kappa = 15$. On the left, the core is AF, while the core is normal on the right.

An important difference between our results and those of Arovav *et al.* is that our solutions have superspin magnitude strictly less than one in the core which allows the transition to be continuous. To see this, let $u = f^2 + m^2$, so u solves the ODE

$$u'' + \frac{1}{r}u' + 2\kappa^2(1-u)u = 2\frac{(1-S)^2}{r^2}f^2 + 2g\kappa^2m^2 + (f')^2 + (m')^2. \quad (10)$$

First, assume that the maximum value of u is achieved at $r_0 \geq 0$. Note that $u'(r_0) = 0$, which follows from standard calculus if $r_0 > 0$, and $u'(0) \leq 0$ if $r_0 = 0$. In addition, $u''(r_0) \leq 0$ and the right-hand side of (10) must be strictly positive at r_0 , so $2\kappa^2(1-u)u > 0$. Since $u \geq 0$ by its definition, we must have $u = f^2 + m^2 < 1$. In the core region, we can say even more. Since m is positive

and decreasing, it attains its maximum at $r = 0$, and therefore (9) implies

$$0 \geq m''(0) = \frac{\kappa^2}{2}(g-1+m(0)^2)m(0).$$

When $m(0) > 0$ we have the upper bound on the AF order parameter at the core:

$$m(r)^2 \leq m(0)^2 \leq 1-g. \quad (11)$$

Since $f(r) \sim r$ for $r \sim 0$, we conclude that the superspin magnitude is bounded by $\sqrt{1-g}$ at $r = 0$.

B. Phase transition

Conventional superconducting vortices with normal cores are obtained by minimizing \mathcal{E} under the constraint $m(r) = 0$. Note that when $m = 0$ equations (7)–(9) reduce to the well-known vortex equations of Abrikosov which have been extensively studied in the physical and mathematical literature. [3,4,6–8]. We denote by $f_{\kappa,0}, S_{\kappa,0}$ these normal-core vortex solutions.

We find that there is a critical value g_κ^* with $0.2 < g_\kappa^* < 0.3$ at which the stability of the normal-core solutions $f_{\kappa,0}, S_{\kappa,0}$ (with $m = 0$) changes: normal cores are stable (i.e., energy minimizing) when $g > g_\kappa^*$ and unstable for $0 < g < g_\kappa^*$. To see this, we linearize (9) at the normal core solution to obtain an eigenvalue problem:

$$\frac{1}{\kappa^2}\tilde{m}''(r) + \frac{1}{\kappa^2r}\tilde{m}'(r) + (1-f_{\kappa,0}^2)\tilde{m} = g\tilde{m}. \quad (12)$$

Define g_κ^* to be the ground-state eigenvalue, with associated eigenstate \tilde{m}_κ . From Rayleigh's principle, \tilde{m}_κ is the minimizer of

$$-g_\kappa^* = \min_{w \neq 0} \frac{\int_0^\infty [\kappa^{-2}(w')^2 - (1-f_{\kappa,0}^2)w^2] r dr}{\int_0^\infty w^2 r dr}, \quad (13)$$

When g crosses below the value g_κ^* , the linearized operator associated with (9) possesses a negative eigenvalue, and the normal core solutions become unstable. In fact, by perturbing the normal core solution $m = 0$ by a small multiple $\epsilon\tilde{m}$ of the eigenstate, we see that the energy is decreased by allowing a nonzero AF component when $g < g_\kappa^*$:

$$\mathcal{E}[f_{\kappa,0}, S_{\kappa,0}, \epsilon\tilde{m}_\kappa] = \mathcal{E}[f_{\kappa,0}, S_{\kappa,0}, 0] + \frac{\epsilon^2}{2}(g-g_\kappa^*)\kappa^2 \int_0^\infty \tilde{m}_\kappa^2 r dr + O(\epsilon^3). \quad (14)$$

Our numerical computations show that the transition is continuous (second order) at g_κ^* . Indeed, in Figure 2 we plot a bifurcation curve, g vs. $m(0)$ obtained by numerical simulation at several values of κ . Since $m(r)$ is a decreasing, positive function, the value $m(0)$ represents

the maximum value of m . Our analytic and numerical results predict that the superspin parameter will lift continuously out of the superconducting plane as g is decreased through the critical value g_κ^* , with its maximum value approaching 1 as $g \rightarrow 0$ from above. In Figure 3 we illustrate the continuous growth of the AF component with decreasing g . We see also that the radius of the vortex core increases as anisotropy g decreases.

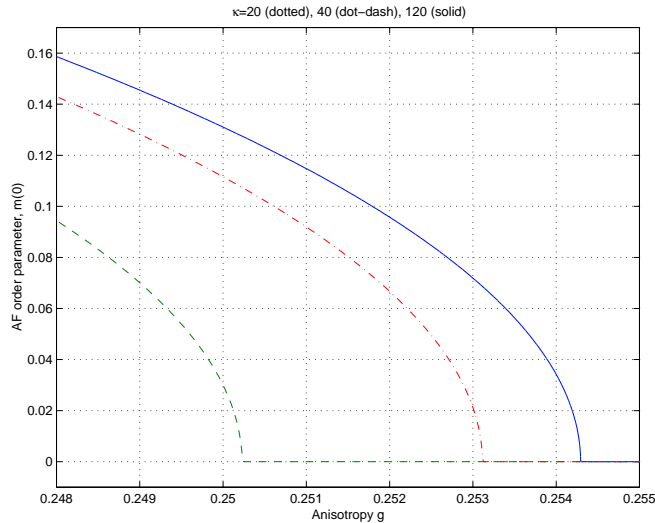


FIG. 2. Nucleation of antiferromagnetic cores for various κ

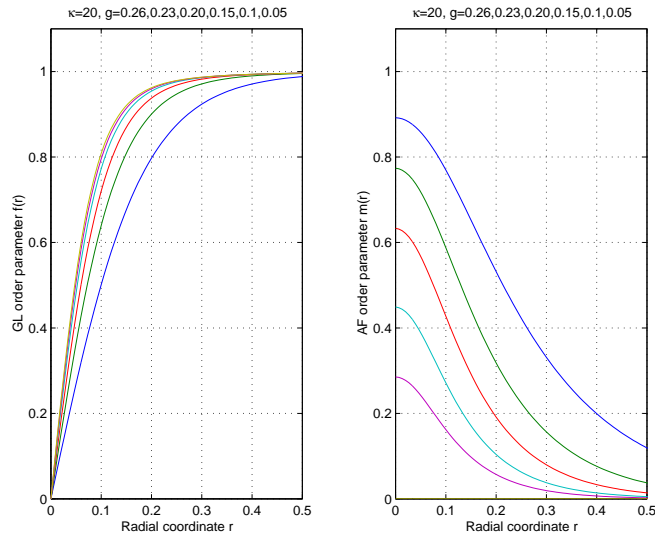


FIG. 3. f, m for different values of g . As g decreases, we see that the radius of the vortex increases and that m increases.

In computing the bifurcation curves shown in Figure 2 we allow g to change very slowly in time, $g(t) \sim 10^{-8} t$. In this way, the minimum point of the free energy moves, but very slowly compared to the relaxation time of the gradient flow. We ran the program with many different values of κ and grid spacings and always observed the same qualitative behavior for the transition. The results

obtained with slowly varying g were checked against solutions calculated at some fixed g and found to be virtually identical. As a further check on our routines we made an independent computation of the bifurcation point g_κ^* using the Rayleigh formula (13). Using a finite element discretization of (13) and a standard eigenvalue solver from EISPACK, we obtain good agreement with the observed transition values in Figure 2. Some values are given in Table II B.

κ	g_κ^*
20	0.2502
40	0.2531
80	0.2541
120	0.2543
∞	0.2545

TABLE I. Values of g_κ^* . Computations were made with 1501 grid points.

Next we consider the dependence on g of the dimensionless vortex-line energy ϵ_1 of an AF core for large κ ($\kappa = 200$). A standard estimate [9] shows that for large κ

$$\epsilon_1 = \frac{1}{4\pi} \mathcal{E} \sim \frac{1}{4} (\ln \kappa + C_1(g)). \quad (15)$$

Our numerics predict a value $C_1(g) = 0.49739$ when $g > g_k^*$ (normal cores), which is in good agreement with the value $C_1 = 0.4976$ obtained by Hu [8]. For AF cores, we observe that $C_1(g)$ decreases as g decreases (*cf.* Figure 4).

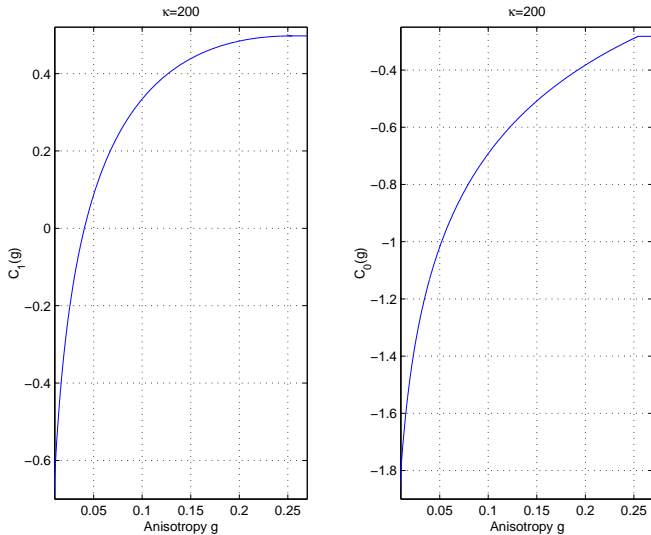


FIG. 4. Dependence of C_1 and C_0 on g

Similarly, for large κ

$$h(0) \sim \ln \kappa + C_0(g) \quad (16)$$

with $C_0(g) = -.28192$ for $g > g_k^*$ (in good agreement with Hu [8] who obtained $C_0 = -.2823$) and with $C_0(g)$ decreasing as g decreases (*cf.* Figure 4). So the values of ϵ_1 and $h(0)$ decrease as the cores becomes more AF. Recall that the size of the core also increases as can be seen in Figure 3. These results show that both H_{c_1} and H_{c_2} decrease as the core becomes larger and more anti-ferromagnetic.

III. THE EXTREME TYPE II LIMIT

To compare our results more directly with the work of Arovas et al [2] we consider the extreme type II model. In fact, for this simpler model we may obtain rigorous analytical results concerning the transition to AF cores. [6] After rescaling by the correlation length $\xi = \kappa^{-1}$, the order parameters converge (uniformly) to a fixed profile, $f_\kappa(\frac{r}{\kappa}) \rightarrow f_\infty(r)$ and $m_\kappa(\frac{r}{\kappa}) \rightarrow m_\infty(r)$ as $\kappa \rightarrow \infty$. (Note that in this scaling $S_\kappa(\frac{r}{\kappa}) \rightarrow 0$.) Passing to the limit in

(7)–(9) we obtain the extreme Type II equations for f_∞ and m_∞ ,

$$-f_\infty'' - \frac{1}{r} f_\infty' + \frac{1}{r^2} f_\infty - (1 - f_\infty^2 - m_\infty^2) f_\infty = 0, \quad (17)$$

$$-m_\infty'' - \frac{1}{r} m_\infty' + g m_\infty - (1 - f_\infty^2 - m_\infty^2) m_\infty = 0. \quad (18)$$

For this model, it is rigorously proven [6] that a continuous phase transition to AF cores occurs at a critical value $g = g_\infty^*$, with g_∞^* the ground-state eigenvalue of the linearized equation (18) at the normal core solution,

$$-g_\infty^* = \min \frac{\int_0^\infty [(w')^2 - (1 - f_\infty^2) w^2] r dr}{\int_0^\infty w^2 r dr} \quad (19)$$

At each value of g there is exactly one stable vortex solution. That stable profile has a normal core when $g \geq g_\infty^*$, and an AF core when $g < g_\infty^*$. In other words, the bifurcation diagrams obtained by numerical simulation of (7)–(9) with κ finite are proven valid for the limiting problem (17), (18). This provides another check on our simulations. For κ large we should see qualitatively similar behavior between this model and that of (17), (18). Numerical computation of g_∞^* using the Rayleigh formula (19) is consistent with the other calculated values of g_κ^* . (See Table II B.) It also shows that vortices with AF cores are stable in a much broader range than was found in Arovas *et al.* [2], where g_∞^* is estimated as 0.0941. This discrepancy is due to the fact that the superspin magnitude is in fact far from 1 in the core region (see our analysis in Section 2.1), while the variational solution of Arovas et al [2] assumes that AF core solutions have superspins constrained to the unit sphere. [10]

IV. PHASE DIAGRAM

The results of the previous two sections for g_κ^* define a region in the phase diagram in which vortices with anti-ferromagnetic cores are stable. To illustrate this statement, we add the (dashed) line for the stability boundary of vortices with anti-ferromagnetic cores to the SO(5) mean-field phase diagram, assuming the relation (5) between g and μ . The result is shown in Figure 5.

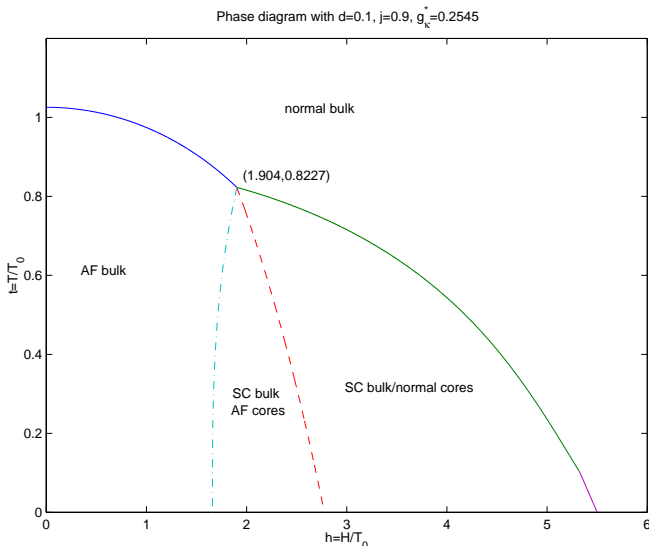


FIG. 5. Mean field phase diagram for the “spin-flop” model defined by Eq. (20). The solid lines separating the AF and SC bulk phases from the high temperature disordered state represent continuous transitions. The dot-dash line separating AF bulk from “SC bulk AF cores” is first order, and the dashed boundary between “AF cores” and “normal cores” represents the continuous transition obtained in this paper.

The SO(5) mean-field phase diagram of Figure 5 is actually the mean field “spin-flop” phase diagram for the three-component antiferromagnet with uniaxial anisotropy in a parallel magnetic field. In this analog system [1], the antiferromagnetic state with its Neel vector parallel to the field corresponds to the SO(5) AF state, while the “flopped” antiferromagnetic state, with Neel vector perpendicular to the applied field, corresponds to the SC state. The field H plays the role of the SO(5) chemical potential μ . The spin Hamiltonian for this system is:

$$\mathcal{H} = J \sum_{(m,n)} [S_m^z S_n^z + j(S_m^x S_n^x + S_m^y S_n^y)] - D \sum_m (S_m^z)^2 - H \sum_m S_m^z. \quad (20)$$

Where $d = D/J$ and j are parameters which control the anisotropy. Figure 5 shows the mean field phase diagram for this model for specific values of these parameters ($d=0.1, j=0.9$). The unit of energy in this diagram is $T_0 = zJ/3$ where z is the coordination number. The region labeled “SC bulk, AF cores” is bounded on the left by the first order SC-to-AF transition and on the right by the stability boundary for AF cores.

At the mean field level one might expect to see antiferromagnetic cores throughout this region, with the amplitude of the antiferromagnetism being largest close to the first order boundary. However, as Bruus *et al* [11] discuss, the spins in the cores are likely to be only weakly correlated from one vortex to the next, and hence the signatures of antiferromagnetic vortex cores may be rather subtle. Bruus *et al* suggest that excitations of the cores

could be studied by inelastic neutron scattering, while Arovas *et al* [2] proposed studying the effect of antiferromagnetic cores on the μ SR spectrum.

V. ACKNOWLEDGEMENTS

This work was supported by the Natural Sciences and Engineering Research Council of Canada. We thank the Brockhouse Institute for Materials Research for supporting a workshop which brought together physicists and mathematicians to discuss issues in superconductivity. AJB acknowledges the hospitality of the Aspen Center for Physics, where part of this paper was written, and support from the Superconductivity Program of the Canadian Institute for Advanced Research.

-
- [1] S.C. Zhang, *Science*, 275:1089, 1997.
 - [2] D.Arovas, J.Berlinsky, C.Kallin, S.C.Zhang, *Phys. Rev. Lett.*, 79:2871, 1997
 - [3] M.S. Berger, Y.Y. Chen, *Jour. Functional Analysis*, vol. 82, 259–295, 1989.
 - [4] B. Plohr, Princeton University PhD Dissertation, 1980.
 - [5] A. Jaffe, C. Taubes, “Vortices and Monopoles,” Birkhäuser, Boston 1980.
 - [6] S. Alama, L. Bronsard, T. Giorgi, preprint math.AP/9903127 v2.
 - [7] A.A. Abrikosov, *Zh. Eksperim. i Teor. Fiz.* **32**, 1442 (1957) [*Sov. Phys.-JETP* **5**,1174 (1957)].
 - [8] C.-R. Hu, *Phys. Rev. B*, vol. 6, 1756–1760, 1972.
 - [9] M. Tinkham, “Introduction to Superconductivity,” McGraw–Hill, New York, 1996.
 - [10] Arovas *et al.* sketched a calculation similar to the above, for a free energy with anisotropic fourth order terms, in Eqs. (8-10) of their paper. However they did not present any numerical results.
 - [11] H. Bruus, K.A. Eriksen, M. Hallundbaek and P. Hede-gard, cond-mat/9807167/.